A TIME DEPENDENT, QUASI-THREE DIMENSIONAL DEPTH-INTEGRATED NUMERICAL MODEL TO CALCULATE SURFACE HEAT TRANSFER AND ENTRAINMENT TO COLD FLUID INTRUSIONS

By
Robert N. Meroney*

Submitted to

International Symposium on Defined Plane Modeling and
Turbulence Measurements, Iowa City, Iowa
16-18 September, 1985

Fluid Mechanics and Wind Engineering
Civil Engineering Department
Colorado State University
Fort Collins, CO 80523

*Professor, Civil Engineering

CEP84-85-RNM12

A TIME DEPENDENT, QUASI-THREE DIMENSIONAL DEPTH-INTEGRATED NUMERICAL MODEL TO CALCULATE SURFACE HEAT TRANSFER AND ENTRAINMENT TO COLD FLUID INTRUSIONS

By Robert N. Meroney

Fluid Mechanics and Wind Engineering Program
Colorado State University
Fort Collins, CO 80523

SUMMARY:

A wind-tunnel validated, depth integrated numerical model is developed to calculate the behavior of heavy and cold fluid intrusions. The model is time dependent, quasi-three dimensional and permits intrusion warming from below due to forced or free convection and entrainment of heat or moisture from above.

1.0 INTRODUCTION:

A depth-integrated numerical model has been developed to help calculate surface heat transfer and entrainment to cold fluid intrusions. This model evolved from depth- or crosswind-averaged forms of the conservation equations of mass, momentum, species, and energy. Submodules permit alternate assumptions for the influence of wind profile, heat transfer, humidity, and fluid entrainment. The construction of these models reflects the philosophy of the models developed by Zeman (14), Colenbrander (2), Morgan, Morris, and Ermak (10); however, there are many differences in detail, and the numerical procedure used here is not similar at all.

The depth-averaged model described below solves the layer-averaged lateral and longitudinal momentum, mass continuity, concentration and enthalpy equations for longitudinally varying depth, width, and cross section averaged densities, temperatures, velocities, and concentrations. The model does not make the Boussinesq assumption; it considers the influence of surface heat transfer, water condensation, friction velocity and surface roughness; and it is computationally simple and fast. A recent modification permits evaluation of molecular dispersion on fluid entrainment. Model constants are tuned to fit the laboratory data of Meroney and Lohmeyer (7) or Neff and Meroney (11). The model is not as flexible or as universal as some of the models reviewed, but then it is also not as complex.

2.0 FORMULATION OF THE LAYER-AVERAGED EQUATIONS:

The layer-averaged equations can be written for two dimensional, radially symmetric, or laterally symmetric geometries. Two dimensional and radially symmetric geometries are discussed by Meroney and Lohmeyer (7, 8). The laterally symmetric form of the equations were first described by Meroney (9).

The formalism for creating layer-averaged conservation equations has been discussed in some detail by Ponce and Yabusaki (12); hence, only a short review of the procedure will be provided here. The layer-averaged value of a mean variable is defined as

$$\bar{\Phi} = \frac{1}{H_0}\int_0^H\int_0^B \Phi(x,y,z) \quad dydz. \tag{1}$$

since mean variables are assumed distributed in a similar manner over the cross section, covariances $\overline{\phi_a \phi_b}$ can be approximated as $\overline{\phi_a \phi_b} = \overline{\phi_a} \cdot \overline{\phi_b}$, and any residuals associated with this approximation are considered effective stresses and are included in diffusion terms. When entrainment takes place across the upper boundary of the cloud, H, then the upper boundary must obey

$$\frac{dH}{dt} + U_T\frac{dH}{dx} = W_T + w_e, \tag{2}$$

where U_T and W_T are the mean horizontal and vertical velocities at H, and w_e is the entrainment rate across the upper boundary. The mean hydrostatic pressure within the layer is found from

$$(p(x) - p_a(H)) = \frac{g}{H_0}\int_0^H\int_0^{z'} (\rho - \rho_a) \quad dz'dz, \tag{3}$$

with the aid of Leibnitz rule the conservation equations can be integrated over the y-z plane cross section areas. For a flow in which the x-axis is aligned with the flow vector the control volume is shown in Figure 1. The final equations developed are nondimensionalized with respect to time, space, density, temperature, and energy scales equal to $H_o^{\frac{1}{2}}(g_o')^{-\frac{1}{2}}$, H_o, ρ_o, $T_a - T_o$, and $c_{po}(T_a - T_o)$ respectively where $g'_o = g(SG_o - 1)$. The final expressions used are:

Width Equation:

If the average width of the flow is B(x), then by analogy to Equation (2) we can define

$$\frac{dB}{dt} + U\frac{dB}{dx} = 2(V_g + v_e), \tag{4}$$

Lateral Momentum Equation:

The fluid will spread laterally due to lateral hydrostatic forces which produce a lateral spread velocity, V_g. The lateral momentum will be retarded by surface drag; hence,

$$\frac{dM}{dt} + \frac{dUM}{dx} = \beta_1 \frac{(R-1)}{(R_0-1)} H^2 - \frac{Cf}{2} RV_g^2(B - B_0(HS)) + \frac{1}{Re_T}\frac{d}{dx}\frac{d(M)}{dx} \tag{5}$$

where $M = RV_gHB$, is twice the local half-section-averaged lateral momentum

(HS) = Heavyside operator (1 over source, 0 otherwise),

$C_f/2$ = surface drag coefficient,

β_1 = hydrostatic pressure constant,

$1/Re_T$ = Small numerical diffusivity to maintain stability, and

$R = 1/((1-\theta T)\ (1-C+C(1-\beta)))$, is an equation of state for local gas density in terms of mass fraction and temperature. When the fluid is incompressible, a different state equation is necessary. For liquid/liquid dispersion the appropriate state equation is simply

$$R = (1-C)(1+\beta_{ca}(T_a-T))+CR_o(1+\beta_{co}(T_o-T))$$

where β_{ca}, β_{co} are ambient and source fluid coefficients of volume expansions.

Mass Conservation Equation:

Variation in the mass flux passing through any section is due to entrainment of ambient fluid across plume boundaries or the result of ground level sources.

$$\frac{dN}{dt} + \frac{dUN}{dx} = w_e B + 2v_e H + RW_0 B_0 + \frac{1}{Re_T} \frac{d}{dx}\left(\frac{d(N)}{dx}\right) \tag{6}$$

where $N = RHB$, is total cross-section averaged mass, and

W_o, B_o = source values of width and boiloff velocity.

Mass Fraction Conservation Equation:

The dense fluid species is conserved as it advects from section to section. Boiloff from a surface pool of cryogenic liquid may add to the local flux values and longitudinal diffusion may decrease the values.

$$\frac{dP}{dt} + \frac{dUP}{dx} + R_0 W_0 B_0 + \frac{1}{Re_T} \frac{d}{dx}\left(\frac{d(P)}{dx}\right) \tag{7}$$

where $P = RCHB$, total cross-section averaged mass fraction, and

R_o = source value of density.

Longitudinal Momentum Equation:

Plume velocity in the downwind direction results from entrainment of ambient momentum from the surrounding shear flow and acceleration caused by hydrostatic gradients in the longitudinal direction. The velocity is decreased by surface drag, injection of zero momentum fluid at the ground surface and longitudinal diffusion.

$$\frac{dK}{dt} + \frac{dUK}{dx} = \frac{\beta_1}{2} \frac{d}{dx}\left(\frac{H^2 B(R-1)}{(R_0-1)}\right)$$
$$- \frac{Cf}{2} RU^2 (B - B_0(HS)) \tag{8}$$
$$+ U_a(w_e B + 2v_e H) + \frac{1}{Re_T} \frac{d}{dx}\left(\frac{d(K)}{dx}\right)$$

where $K = RUHB$, total cross-section averaged longitudinal momentum,

$U_a = 1/k\ Ri_*^{\frac{1}{2}} \ln (H/z_o + 1)$, is the ambient shear layer velocity at cloud height,

Enthalpy Conservation Equation:

Sensible energy carried with the plume varies with surface sources and longitudinal dispersion. For dense liquids intruding beneath another liquid the humidity terms are, of course, not used.

$$\frac{dQ}{dt} + \frac{dUQ}{dx} = R_0 E_0 W_0 B_0 + E_a(w_e B + 2v_e H)$$
$$+ h_s T(B - B_0\ (HS)) + \frac{1}{Re_T} \frac{d}{dx}\left(\frac{d(Q)}{dx}\right) \tag{9}$$
$$+ (HS)\ (L_h)\ (\omega_{\phi,T_a} - \omega_{100,T}$$
$$(w_e B + 2v_e H - R_0 W_0 B_0)$$
$$+ (HS)\ (L_h) RB(1 - C)\omega_{100,T} \frac{4886.}{T^2}\ (T_a - T_0)\ \frac{dT}{dx}$$

where $Q = REHB$, total section enthalpy,

$E = -(1+Cs_m)T/(1+s_m)$, is the local cross-section averaged enthalpy,

W, Φ, T = water vapor mass fraction at relative humidity, Φ, and temperature, T,

$L_h = (\ell_{H_2O})/(c_{po}(T_a-T_o)$, is the latent heat of vaporization of water,

$$h_s = 0.32 \left(\frac{Gr}{Re^3 Pr}\ Ri*\right)^{\frac{1}{2}} \frac{(1+Cs_m)}{(1 + s_m)}\ RT^{\frac{1}{2}}$$

is the local surface heat transfer coefficient,

$\beta = 1 - M_a/M_o$, is a dimensionless source molecular weight,

$\theta = 1 - T_o/T_a$, is a dimensionless source temperature,

$s_m^* = c_{po}/c_{pa}-1$, is a dimensionless source specific heat capacity, and

Gr, Re, Pr, Ri_* = Grashof, Reynolds, Prandtl and Richardson number scales, respectively.

An equation of state for gases which relates mass fraction, C, to molar or volume fraction, χ, is also useful.

$$\chi = C(1-\beta)/(1 - C + C(1-\beta)) \tag{10}$$

Such an expression is generally inappropriate for liquid intrusions.

2.1 Water Condensation and Surface Flux Algorithm:

The last two expressions in Equation (9) adjust for heat initially released when a cold gas entrains water vapor, but which is subsequently re-evaporated when the temperature of the plume exceeds ambient dew point. The relations only condense water vapor which exceeds the local saturation values. In these two terms (HS) is the Heavyside operator which equals one when T $T_{dewpoint}$ and zero otherwise. The dimensionless heat transfer coefficient, h_s, is based on the bulk transfer coefficient for mixed free and forced convection recommended by Leovy (6). alternative values for fully forced or fully free convection can also be used.

2.2 Entrainment Algorithms:

Entrainment rates are perturbations on the forms suggested by Eidsvik (4) and Ermak et al. (5). Some other forms tried are reviewed in Meroney and Lohmeyer (8). The recommended entrainment expressions are:

$$w_e = c_z V_g + \frac{\alpha_4 v_*}{\frac{\alpha_4}{\alpha_6} \frac{Ri_*}{RH^2}} \tag{11}$$

$$v_e = \frac{3.24 H v_*}{B} \tag{12}$$

$$v_*^2 = \frac{\alpha^2 \, Gr \, (1+s_m) \, (1-\theta T)}{Re^2 (1+Cs_m) \, (1-\theta)} \quad H h_s T^{2/3} \tag{13}$$

These relations retain a near source term which produces entrainment due to gravity spreading in a calm environment. Expressions by Zeman (14) and Morgan et al. (10) also allow for such a condition. A major difference here is all unspecified constants are determined by comparison to the laboratory data of Meroney and Lohmeyer (7, 8) and Neff and Meroney (11), but once the values were chosen they were not varied during the exercises discussed in Section 4.0.

3.0 NUMERICAL METHOD (DENS22):

Equations (4) to (9) were developed in a difference form using an implicit, second-upwind-difference, donor-cell approach. The difference equations were solved by the Thomas or tri-diagonal algorithm. Step sizes in time were limited to

$$\Delta t < \frac{0.25 \Delta x}{u_{max} + c_{max}}$$

where c_{max} is the maximum local wave speed, and the wave speed is defined as $c = (g'H)^{\frac{1}{2}}$. The algorithms maintained accurate conservation of the original cloud mass. The calculations lost less than 0.5% of the mass over the integration periods studied, primarily due to round-off errors.

Constants found to fit the wind-tunnel data most satisfactorily are $c_z = 0.05$, $\alpha_2 = 0.5$, $\alpha_3 = 1.0$, $\alpha_4 = 2.4$, $\alpha_6 = 0.3$, $\beta_1 = 0.153$, $Cf/2 = 0.0025$ and $1/Re_T = 0.05$.

4.0 VALIDATION EXAMPLES:

The credibility of a numerical model depends upon its ability to reproduce accurately the values of intrusion size and concentration distribution found during experiments. The data selected for comparison to the DENS22 program include instantaneous releases of cold propane and liquid natural gas (LNG) spills on water.

DENS22 Model Comparisons with Maplin Sands Field Experiment:

In 1980 Shell Research, Ltd., performed a series of 34 spills of up to $20m^3$ of liquefied natural gas (LNG) or refrigerated liquid propane onto the sea at Maplin Sands in the south of England (Colenbrander and Puttock, (3)). Release of the cryogenic liquids was either continuous or instantaneous. Continuous spills involved the release of liquid at a steady rate from the end of a pipe near the water surface. For instantaneous spills the liquid was poured into an open-topped insulated barge, 12.5m across, which was then rapidly submerged. Tests from the series were chosen in which heat transfer and latent heat release effects were expected to be significant.

Table I gives data for the conditions which existed during the Maplin Sands experiments, and Table II reports downwind distances to the lower flammability limit (LFL). The LFL location is that distance downwind where, during steady conditions, the peak concentration measured at the lowest sensor level (about 0.9m) dropped below the ignition concentration of the gas. For propane and methane this would be mole fractions of 0.021 and 0.05 respectively. Since these experiments are single replications and uncertainty levels are high the estimated deviations are also tabulated. Maximum concentrations versus downwind distance for LNG spill 29 and Propane spill 43 are shown in Figures 2 and 3. Slab model width predictions are displayed on Figures 4 and 5.

Table II tabulates computed LFL distances for each run predicted by a box model (DENS 6, Andreiev et al., (1)), by HEGADAS (Colenbrander, (2)), and DENS22. A linear regression between experimental and calculated values reveals correlation coefficients for DENS6, HEGADAS, and DENS22 OF 0.77, 0.62, AND 0.69, respectively. If Maplin Sands Run 54 is eliminated as an outlier, the correlations become 0.83, 0.69, and 0.81, respectively.

During all calculations for DENS6 and DENS22 an average value of $u_*/u_{10} = 0.034$ was assumed as recommended by Colenbrander and Puttock (3). The surface roughness magnitude was selected to reproduce measure velocities at one meter assuming the associated friction velocity, U_*. If measured values of u_* at the 10 meter height are used during calculations the correlations improves to r = 0.72 for all runs and to r = 0.89 eliminating Run 54. Scatter diagram plots reveal there is a slight tendency to systematically over-estimate LFL distances for the propane spills and under-estimate LFL distances for the LNG spills.

5.0 SUMMARY AND CONCLUSIONS:

The depth-integrated model (DENS22) was found to reproduce the essence of intrusion behavior for cold dense gas clouds released suddenly, over a finite time, or continuously. The program is reasonably simple (350 lines of Fortran code including print and plot statements), is fast (320 time steps forward in 110 cpu time on a CDC CYBER 185 computer), and does not occupy a large amount of computer memory (a version of the program written in FORTRAN occupies less than 64 k on an IBM PC microcomputer).

REFERENCES:

1. Andreiev, G., Neff, D. E., and Meroney, R. N. (1983), Heat Transfer Effects During Cold-Dense Gas Dispersion, Gas Research Institute Report No. GRI 83/0082, Chicago, IL, USA, 241 pp.
2. Colenbrander, G. W. (1980), A Mathematical Model for the Transient Behavior of Dense Vapour Clouds, 3rd Int. Symp. on Loss Prevention and Safety Promotion in the Process Industries, Basel, Switzerland, 29 pp.
3. Colenbrander, G. W. and Puttock, J. S. (1984), Maplin Sands Experiments 1980: Interpretation and Modeling of Liquified Gas Spills onto the Sea, Proceedings of IUTAM Symposium Delft 1983 on Atmospheric Dispersion of Heavy Gases and Small Particles, Springer Verlag, Berlin, pp. 177-295.
4. Eidsvik, K. J. (1980), A Model for Heavy Gas Dispersion in the Atmosphere, Atmospheric Environment, Vol. 14, pp. 769-777.
5. Ermak, D. L. et al. (1982), A Comparison of Dense Gas Dispersion Model Simulations with Burro Series LNG Spill Test Results, J. Hazardous Materials, Vol. 6, Nos. 1 and 2, pp. 129-160.
6. Leovy, C. B. (1969), Bulk Transfer Coefficient for Heat Transfer, J. of Geophysical Research, Vol. 74, No. 13, pp. 3313-3321.]
7. Meroney, R. N. and Lohmeyer, A. (1982), Gravity Spreading and Dispersion of Dense Gas Clouds Released Suddenly into a Turbulent Boundary Layer, Gas Research Institute Report GRI 81/0025, Chicago, IL, USA, 220 pp.
8. Meroney, R. N. and Lohmeyer, A. (1983), Prediction of Propane Cloud Dispersion by a Wind-tunnel-data Calibrated Box Model, accepted by J. Hazardous Materials, 33 pp.
9. Meroney, R. N. (1984), Transient Characteristics of Dense Gas Dispersion-Part I: A Depth-averaged Numerical Model, J. Hazardous Materials, Vol. 9, pp. 139-157.
10. Morgan, D. L., Jr., Morris, L. K., and Ermak, D. L. (1983), SLAB: A Time-Dependent Computer Model for the Dispersion of Heavy Gases Released in the Atmosphere, Lawrence Livermore National Laboratory, Livermore, CA, Report UCRL-53383, 15 pp.
11. Neff, D. E. and Meroney, R. N. (1982), The Behavior of Heavy Plume Dispersion, Gas Research Institute Report GRI 80/0145, Chicago, IL, USA, 120 pp., (Data Appendix is GRI 80/0145.1, 161 pp.)

12. Ponce, V. M. and Yabusaki, S. B. (1980), Mathematical Modeling of Circulation in Two-dimensional Plane Flow, National Science Foundation Final Report, Grant No. CME7805458, 131 pp.
13. Sokolnikoff, I. S. and Redheffer, R. M. (1958), Mathematics of Physics and Modern Engineering, McGraw Hill Pub. Co., New York, 812 pp.
14. Zeman, O. (1982), The Dynamics and Modeling of Heavier-than-air, Cold Gas Releases, Atmospheric Environment, Vol. 16, No. 4, pp. 741-751.

MAPLIN SANDS 1980 DISPERSION TRIALS
DATA SUMMARY

SPILL NO.	Rio	RATE liq (m3/m)	RATE gas (m3/s)	DURATION (sec)	Wo (m/s)	Ro (m)	U10 (m/s)	U1 (m/s)	To (oC)	T10 (oC)	T2 (oC)	HUMIDITY %	* U* 10 (m/s)	* U* 1 (m/s)	* (U*/U)10	** (u*)avg (m/s)	** Zo (m)	*** (u*)vel (m/s)	*** Zo (m)
CONTINUOUS PROPANE																			
42	103.0	2.5	10.4	180.0	0.050	14.4	3.7	2.9	-40.0	18.3	18.3		0.13	0.07	0.035	0.126	1.00E-04	0.148	4.44E-04
43	17.8	2.3	7.6	220.0	0.050	13.8	5.5	3.9	-40.0	16.9	17.0		0.25	0.09	0.045	0.187	2.38E-04	0.276	3.47E-03
46	15.9	2.8	11.7	260.0	0.050	15.3	8.1	7.1	-40.0	13.7	13.7	71.0	0.23	0.27	0.028	0.275	3.30E-05	0.174	7.94E-08
47	55.7	3.9	16.2	210.0	0.050	18.0	5.6	4.8	40.0	17.4	17.4	78.0	0.16	0.20	0.029	0.170	4.00E-05	0.129	1.00E-06
49	21.1	2.0	8.3	90.0	0.050	12.9	6.2	5.5	-40.0	13.1	13.3	88.0	0.21	0.21	0.034	0.211	3.00E-05	0.122	1.29E-08
50	12.0	4.3	17.9	160.0	0.050	18.9	7.9	6.0	-40.0	10.3	10.4	79.0	0.29		0.037	0.269	1.30E-04	0.330	6.95E-04
52	3.3	5.3	22.1	140.0	0.050	21.0	7.9	5.8	-40.0	11.9	11.8	63.0	0.59		0.075	0.269	1.80E-04	0.365	1.70E-03
54	59.0	2.3	9.6	180.0	0.050	13.8	3.8	3.0	-40.0	8.4	8.4	85.0	0.16		0.042	0.129	9.10E-05	0.139	1.79E-04
CONTINUOUS LNG																			
9	1.2	1.6	6.4	200.0	0.048	11.6	8.9	7.0	-162.0	16.4	16.7	84.0	0.48	0.30	0.054	0.303	9.70E-05	0.330	2.07E-04
12	335.4	0.9	3.6	240.0	0.048	8.7	1.5	1.5	-162.0		14.6	91.0	0.06	0.09	0.040	0.051	7.80E-06		
15	141.9	2.9	11.7	225.0	0.048	15.6	3.6	3.2	-162.0	15.1	15.7	88.0	0.08	0.11	0.022	0.122	2.80E-05	0.069	1.60E-08
27	ERR	3.2	12.9	160.0	0.048	16.4	5.5		-162.0			53.0	0.25	0.19	0.045	0.187	7.80E-05		
29	8.4	4.1	16.5	225.0	0.048	18.5	7.4	6.5	-162.0	16.0	16.1	52.0	0.35	0.20	0.034	0.252	3.30E-05	0.155	4.85E-08
34	5.3	3.0	12.1	95.0	0.048	15.9	8.6	7.7	-162.0	14.9	15.2	72.0	0.27	0.28	0.031	0.292	2.60E-05	0.149	1.00E-09
35	6.7	3.8	15.3	135.0	0.048	17.8	9.8	8.5	-162.0	15.6	16.1	63.0	0.24	0.31	0.024	0.333	3.50E-05	0.221	1.92E-07
39	21.4	4.7	18.9	60.0	0.048	19.9	4.1	3.1	-162.0	16.9	16.7	63.0	0.22	0.08	0.054	0.139	1.30E-04	0.174	7.94E-04
56	18.8	2.5	10.1	80.0	0.048	14.5	5.1	3.9	-162.0	13.5	14.6	83.0	0.17		0.034	0.173	1.20E-04	0.212	6.60E-04

Table 1: Maplin Sands 1980 Dispersion Trials
Data Summary

* Flux Measurements

** Assume $u_*/u_{10} = 0.034$

*** Calculate u_* and Zo from logarithmic velocity profile fit to velocity data

SPILL NO.	LFL (m)	** LFL HEGADAS (m)	** LFL dens6 (m)	** LFL dens22 (m)	*** LFL dens22 (m)
CONTINUOUS PROPANE					
42	220+-25	315	322	283	273
43	215+-20	245	270	270	216
46	245+-35	225	248	300	426
47	340+-90	320	370	378	414
49	285+-25	210	234	296	362
50	210+50-25	280	270	371	321
52	200+-30	315	315	385	315
54	450+-70	295	314	280	271
CONTINUOUS LNG					
9	135+-15	90	120	77	77
12	63+-4	45	70	52	52
15	165+-15	100	155	100	184
27	190+-20	225	245	119	119
29	140+-15	245	170	120	137
34	150+-20	165	190	105	133
35	175+-25	205	210	124	133
39	120+-20	290	215	110	112
56	110+-30	115	140	90	65
Correl. Coeff., r =		0.62	0.77	0.69	0.72
no Run 54 r =		0.69	0.83	0.81	0.89

Table 2: Distances to Lower Flammability Limit for Maplin Sands Cold Gas Intrusion Tests

** Assume $u_*/u_{10} = 0.034$

*** Calculate u_* and Zo from logarithmic velocity profile fit to velocity data

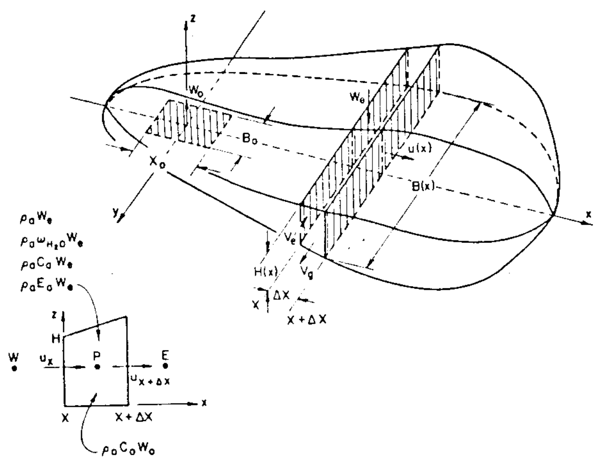

Figure 1: Central volume for depth-averaged transport equations

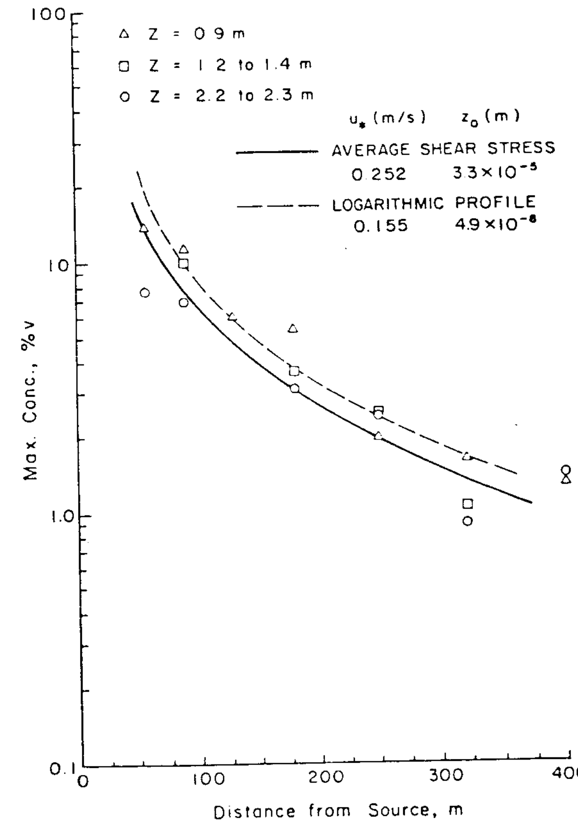

Figure 2: Maximum surface concentrations versus downwind distances for LNG spill, Run 29, at Maplin Sands

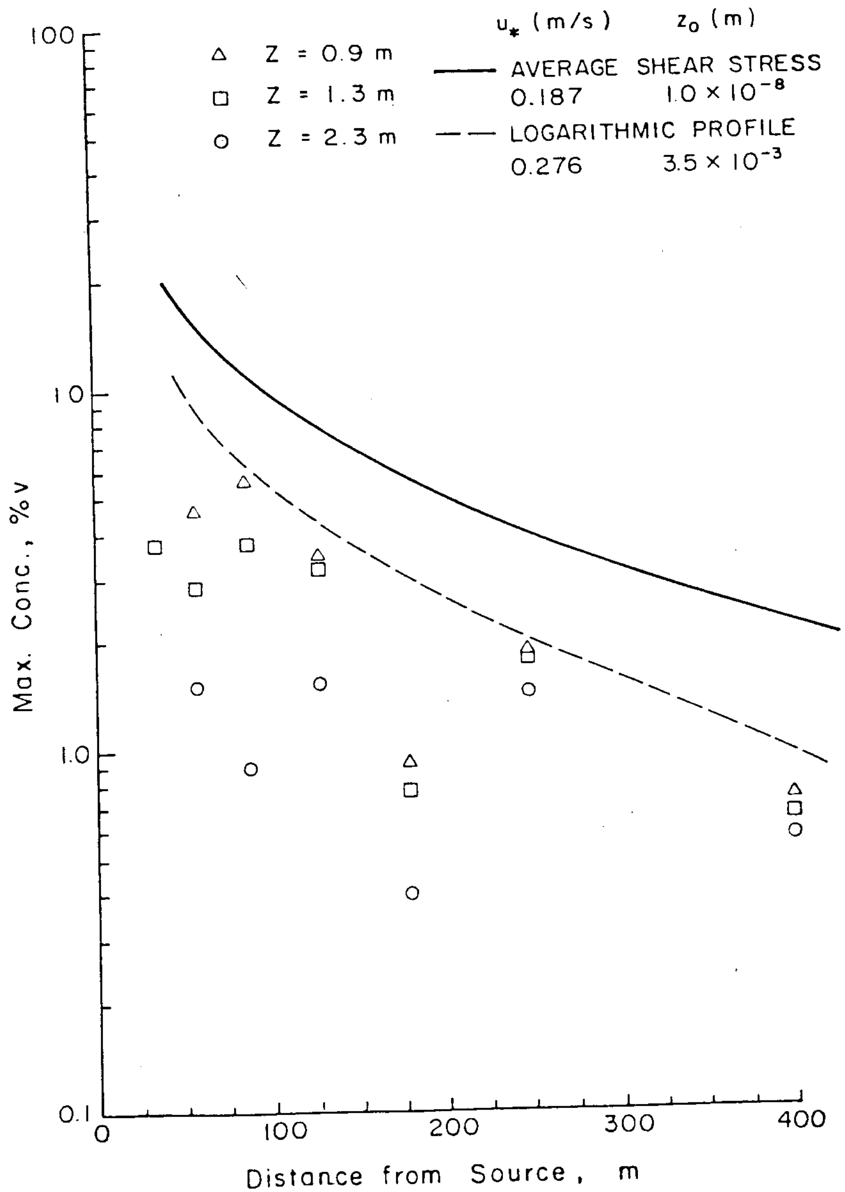

Figure 3. Maximum surface concentrations versus downwind distances for Propane Spill, Run 43, at Maplin Sands.

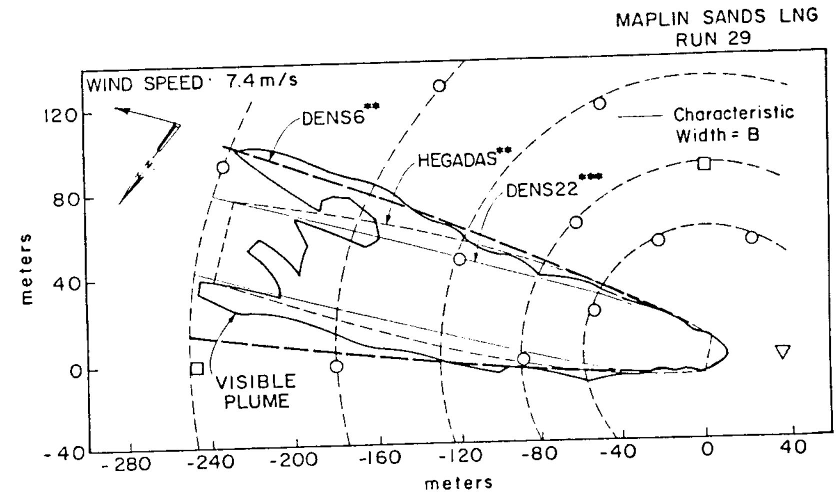

Figure 4: Plan view for LNG Spill, Run 29, at Maplin Sands

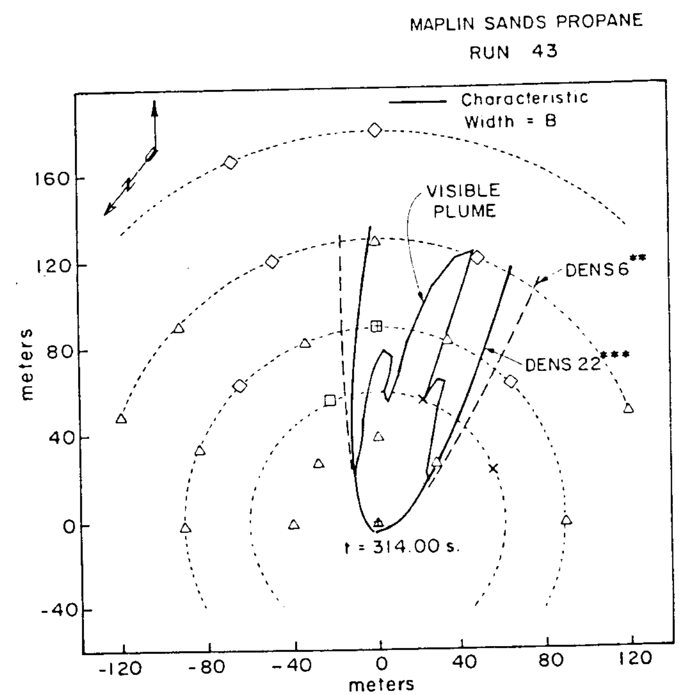

Figure 5: Plan view for Propane Spill, Run 43, at Maplin Sands

KEY WORDS

Heat transfer
Dense gas dispersion
Fluid intrusions
Numerical model